

ERROR ESTIMATES FOR THE ARNOLDI APPROXIMATION OF A MATRIX SQUARE ROOT*

JAMES H. ADLER[†], XIAOZHE HU[†], WENXIAO PAN[‡], AND ZHONGQIN XUE[†]

Abstract. The Arnoldi process provides an efficient framework for approximating functions of a matrix applied to a vector, i.e., of the form $f(M)\mathbf{b}$, by repeated matrix-vector multiplications. In this paper, we derive an *a priori* error estimate for approximating the action of a matrix square root using the Arnoldi process, where the integral representation of the error is reformulated in terms of the error for solving the linear system $M\mathbf{x} = \mathbf{b}$. The results extend the error analysis of the Lanczos method for Hermitian matrices in [Chen et al., SIAM J. Matrix Anal. Appl., 2022] to non-Hermitian cases. Furthermore, to make the method applicable to large-scale problems, we assume that the matrices are preprocessed utilizing data-sparse approximations preserving positive definiteness, and then establish a refined error bound in this setting. The numerical results on matrices with different structures demonstrate that our theoretical analysis yields a reliable upper bound. Finally, simulations on large-scale matrices arising in particulate suspensions validate the effectiveness and practicality of the approach.

Key words. Arnoldi approximation, matrix square root, matrix functions

MSC codes. 65F60 65Z05 70-10

1. Introduction. Given a matrix $M \in \mathbb{C}^{n \times n}$, its square roots are the solutions of $X^2 = M$. If M is positive definite, then M admits a unique positive definite square root [19], denoted as $M^{1/2}$. Matrix square roots frequently arise in stochastic simulation [12], state estimation [2], image reconstruction [3], and Bayesian optimization [31, 18]. Hence, the computation of a matrix square root is a fundamental problem in numerical linear algebra.

There are a list of approaches in the literature for computing the square root of a matrix. Cholesky decomposition and eigenvalue decomposition provide useful tools for symmetric positive definite (SPD) matrices [35]. For general matrices, the Schur decomposition transforms the matrix into a triangular form, where the square root can be computed explicitly [19]. Additionally, Newton-like iterations [19] provide stable and efficient implementation for approximating the matrix square root. Unfortunately, these classical methods all suffer from at least $\mathcal{O}(n^3)$ complexity for large-scale matrices [19]. On the other hand, even when M is sparse or structured, its square root is typically dense, making direct computation and storage costly or even infeasible for large-scale problems. Consequently, rather than computing the square root of a matrix explicitly, the main interest lies in computing the action of a matrix square root on a vector. This is also the case for general matrix functions. Krylov subspace methods such as the Arnoldi iteration, therefore provide a powerful framework, as they only rely on repeated matrix-vector multiplications to construct the Krylov subspace. For general dense matrices, the overall computational cost of the Arnoldi process is about $\mathcal{O}(kn^2)$, where k is the number of Arnoldi iterations. When the matrix is Hermitian, the Arnoldi process simplifies to the Lanczos algorithm, characterized by a three-term recurrence. Strategies such as restarting [13, 15, 20],

*Submitted to the editors DATE.

Funding: This work was funded by NSF DMS-2208267 and ARO W911NF2310256

[†]Department of Mathematics, Tufts University, Medford, MA 02155, USA (James.Adler@tufts.edu, Xiaozhe.Hu@tufts.edu, Zhongqin.Xue@tufts.edu).

[‡]Mechanical Engineering, University of Wisconsin-Madison, Madison, WI 53706, USA (wpan9@wisc.edu).

truncated orthogonalization [30, 9], and randomized sketching [30, 9, 29, 16] have been explored to reduce memory and orthogonalization cost.

Recently, there has been growing interest in the theoretical analysis of Krylov methods for approximating the action of matrix functions. As shown in [6], the error of the Lanczos algorithm after k iterations for approximating $f(M)\mathbf{b}$ is bounded by the error of the best k -degree polynomial that uniformly approximates $f(x)$ over the spectral interval $[\lambda_{\min}(M), \lambda_{\max}(M)]$, where $\lambda_{\min}(M)$ and $\lambda_{\max}(M)$ denote the smallest and largest eigenvalues of the matrix M , respectively. Such a classical bound has also been studied within the setting of finite precision arithmetic [28]. In [11], *a posteriori* error estimates for polynomial Krylov methods are developed and applied to a broad class of matrix functions with integral representations. Based on the Cauchy integral formula, Chen et al. [6] establish *a priori* and *a posteriori* error bounds for the Lanczos method by reformulating the approximation error in terms of the error of solving a shifted linear system. In addition, the authors in [1] explore the near optimality of the Lanczos methods for rational functions with real poles lying outside the spectral interval of M . Their results are established under the assumption that the matrices are Hermitian, while in many practical applications, the matrices of interest are non-Hermitian. This motivates us to extend their results to the non-Hermitian setting.

In this work, we present an *a priori* error bound of the Arnoldi process specifically for evaluating a matrix square root, extending the results in [6] to the case of positive-definite non-Hermitian matrices. The main idea is to utilize the integral representation of the error in the iterations of the Arnoldi process, and then relate it to the error for solving the linear system $M\mathbf{x} = \mathbf{b}$. Compared to Hermitian matrices, non-Hermitian matrices exhibit complex spectral behavior: they are not necessarily diagonalizable, and even when they are, the eigenvectors are typically not orthogonal and the eigenvalues may be complex. To address these difficulties, we employ two techniques: the first is applying the Cauchy integral formula to estimate the norms of matrix functions for general matrices that may not be diagonalizable; the second is relating the modulus of a function in the complex plane to the real-valued function of the modulus, reducing the analysis to the positive real line. Moreover, for large-scale problems, we derive an error bound for approximating the matrix square root based on a data-sparse representation of the matrix. In numerical experiments, we investigate matrices with different structures to verify the theoretical results. Furthermore, we validate the effectiveness of our approach on large-scale mobility matrices arising from particulate suspension simulations. To improve computational efficiency and reduce storage cost, the matrices are preprocessed through adaptive cross approximation and stored in the form of hierarchical matrices.

The remainder of this paper is arranged as follows. In Section 2, we introduce the Arnoldi process for matrix functions. Error estimation of the Arnoldi process for computing a square root is provided in Section 3. Section 4 presents the implementation and reports our numerical results. Finally, concluding remarks are made in Section 5.

2. Matrix functions and Arnoldi iterations. There are different ways to define a function of a matrix, depending on the properties of the matrix and the type of function. In this work, we focus on two of them: the definition via the Jordan canonical form and the Cauchy integral representation.

Given a square matrix $M \in \mathbb{C}^{n \times n}$, assume its Jordan canonical form is given by

$$M = ZJZ^{-1},$$

where Z is a nonsingular matrix, and $J = \text{diag}(J_1, J_2, \dots, J_p)$ with $J_k \in \mathbb{R}^{m_k}$, $\sum_{i=1}^p m_k = n$ being a Jordan block associated with the eigenvalue λ_k , $1 \leq k \leq p$. Then, the matrix function $f(M)$ is defined as

$$f(M) := Zf(J)Z^{-1} = Z \text{diag}(f(J_1), f(J_2), \dots, f(J_p))Z^{-1},$$

where $f(J_k)$ takes the form:

$$(2.1) \quad f(J_k) := \begin{bmatrix} f(\lambda_k) & f'(\lambda_k) & \dots & \frac{f^{(m_k-1)}(\lambda_k)}{(m_k-1)!} \\ & f(\lambda_k) & \ddots & \vdots \\ & & \ddots & f'(\lambda_k) \\ & & & f(\lambda_k) \end{bmatrix}.$$

Alternatively, when f is analytic on a domain containing the spectrum of M , one can also define $f(M)$ using the Cauchy integral formula:

$$f(M) = -\frac{1}{2\pi i} \int_{\mathcal{C}} f(z)(M - zI)^{-1} dz,$$

where \mathcal{C} is a closed contour enclosing the spectrum of M . The two definitions are equivalent when f is analytic [19].

Algorithm 2.1 Arnoldi Process

```

1: Input: Matrix  $M \in \mathbb{C}^{n \times n}$ , vector  $\mathbf{b} \in \mathbb{C}^n$ , and iteration number  $k$ 
2: Initialize: Set  $\mathbf{q}_1 = \mathbf{b}/\|\mathbf{b}\|$  and  $Q_k = [\mathbf{q}_1]$ 
3: for  $j = 1$  to  $k$  do
4:    $\mathbf{w} = M\mathbf{q}_j$ 
5:   for  $i = 1, \dots, j$  do
6:      $h_{i,j} = \mathbf{q}_i^* \mathbf{w}$ 
7:      $\mathbf{w} = \mathbf{w} - h_{i,j} \mathbf{q}_i$ 
8:   end for
9:    $h_{j+1,j} = \|\mathbf{w}\|$ 
10:  if  $h_{j+1,j} = 0$  then
11:    Stop
12:  end if
13:   $\mathbf{q}_{j+1} = \mathbf{w}/h_{j+1,j}$ 
14:  Append  $\mathbf{q}_{j+1}$  to  $Q_k = [\mathbf{q}_1, \dots, \mathbf{q}_{j+1}]$ 
15: end for
```

In practice, we are primarily interested in the action of a matrix function $f(M)$ on a vector \mathbf{b} . To achieve this efficiently, we employ the Arnoldi process, which is described in Algorithm 2.1. Given $\mathbf{b} \in \mathbb{C}^n$, this yields

$$(2.2) \quad MQ_k = Q_k H_k + h_{k+1,k} \mathbf{q}_{k+1} \mathbf{e}_k^T,$$

where $H_k = [h_{i,j}] \in \mathbb{C}^{k \times k}$ is an upper Hessenberg matrix satisfying $Q_k^* M Q_k = H_k$, \mathbf{e}_k is the k -th canonical basis vector, and Q_k is an orthonormal matrix whose columns, \mathbf{q}_i , form a basis for the k -th Krylov space,

$$\mathcal{K}_k(M, \mathbf{b}) = \text{span}\{\mathbf{b}, M\mathbf{b}, M^2\mathbf{b}, \dots, M^{k-1}\mathbf{b}\}.$$

Then, the k -th Arnoldi iteration for approximating $f(M)\mathbf{b}$ is given by

$$f(M)\mathbf{b} \approx \text{Arn}_k(f; M, \mathbf{b}) := Q_k f(H_k) Q_k^* \mathbf{b} = \|\mathbf{b}\| Q_k f(H_k) \mathbf{e}_1.$$

Note that when $f(x) = 1/x$, the Arnoldi approximation reduces to the Full Orthogonalization Method (FOM) [33] for solving the linear system $M\mathbf{x} = \mathbf{b}$, with initial guess $\mathbf{x}_0 = \mathbf{0}$. For the rest of this paper, whenever FOM is referred, we always assume the initial guess is zero.

3. Error bound. In this section, we study an *a priori* error bound of the Arnoldi process for approximating general matrix functions and then focus on the analysis of the matrix square root.

3.1. Integral representation of the error. Let f be analytic along and inside a contour \mathcal{C} that encloses the spectrum of both M and H_k . By the Cauchy integral representation of $f(H_k)$, the k -th Arnoldi approximation to $f(M)\mathbf{b}$ is given by:

$$\text{Arn}_k(f; M, \mathbf{b}) = \|\mathbf{b}\| Q_k f(H_k) \mathbf{e}_1 = -\frac{\|\mathbf{b}\|}{2\pi i} \int_{\mathcal{C}} f(z) Q_k (H_k - zI)^{-1} \mathbf{e}_1 dz.$$

The integral involves solving a shifted linear system $(M - zI)\mathbf{x} = \mathbf{b}$ using FOM, yielding the approximation $\|\mathbf{b}\| Q_k (H_k - zI)^{-1} \mathbf{e}_1$. The corresponding error and residual are defined as:

$$\boldsymbol{\xi}_z^k := (M - zI)^{-1} \mathbf{b} - Q_k (H_k - zI)^{-1} \|\mathbf{b}\| \mathbf{e}_1 \quad \text{and} \quad \mathbf{r}_z^k := (M - zI) \boldsymbol{\xi}_z^k.$$

Then, we represent the error of the Arnoldi process for $f(M)\mathbf{b}$ by:

$$(3.1) \quad f(M)\mathbf{b} - \text{Arn}_k(f; M, \mathbf{b}) = f(M)\mathbf{b} - \|\mathbf{b}\| Q_k f(H_k) \mathbf{e}_1 = -\frac{1}{2\pi i} \int_{\mathcal{C}} f(z) \boldsymbol{\xi}_z^k dz.$$

LEMMA 3.1. *For $z \in \mathbb{C}$ lying on a closed contour \mathcal{C} that encloses the spectrum of H_k ,*

$$\mathbf{r}_z^k = \left(\frac{(-1)^k}{\det(H_k - zI)} \prod_{j=1}^k h_{j+1,j} \right) \|\mathbf{b}\| \mathbf{q}_{k+1}.$$

Proof. According to Algorithm 2.1, we have

$$(M - zI)Q_k = Q_k(H_k - zI) + h_{k+1,k} \mathbf{q}_{k+1} \mathbf{e}_k^T,$$

and then,

$$\begin{aligned} \|\mathbf{b}\| (M - zI) Q_k (H_k - zI)^{-1} \mathbf{e}_1 &= Q_k \|\mathbf{b}\| \mathbf{e}_1 + h_{k+1,k} \mathbf{q}_{k+1} \mathbf{e}_k^T (H_k - zI)^{-1} \|\mathbf{b}\| \mathbf{e}_1 \\ &= \mathbf{b} + \|\mathbf{b}\| h_{k+1,k} \mathbf{q}_{k+1} \mathbf{e}_k^T (H_k - zI)^{-1} \mathbf{e}_1. \end{aligned}$$

Noting that $(H_k - zI)^{-1} = (1/\det(H_k - zI)) \text{adj}(H_k - zI)$ and using the properties of an adjugate matrix leads to

$$\mathbf{e}_k^T (H_k - zI)^{-1} \mathbf{e}_1 = \frac{\text{cof}(H_k - zI)_{1k}}{\det(H_k - zI)} = \frac{(-1)^{k+1}}{\det(H_k - zI)} \prod_{j=1}^{k-1} h_{j+1,j},$$

where $\text{cof}(H_k - zI)_{1k}$ denotes the $(1, k)$ -cofactor of $H_k - zI$. Substituting this into the expression for \mathbf{r}_z^k gives the desired result. \square

Applying [Lemma 3.1](#), we establish the following result, which connects the errors and residuals of the Arnoldi approximations for different shifts.

LEMMA 3.2. *Assuming M and $M - zI$ are invertible for some $z \in \mathbb{C}$, we obtain*

$$\boldsymbol{\xi}_z^k = \det(h_z(H_k))h_z(M)\boldsymbol{\xi}_0^k \quad \text{and} \quad \mathbf{r}_z^k = \det(h_z(H_k))\mathbf{r}_0^k,$$

where the function $h_z(x)$ is defined as $h_z(x) := (x - z)^{-1}x$.

Proof. The proof follows a similar argument to that of Corollary 2.4 in [\[6\]](#). \square

Then, we have the following Theorem.

THEOREM 3.3. *Given a nonsingular matrix $M \in \mathbb{C}^{n \times n}$ and a vector $\mathbf{b} \in \mathbb{C}^n$, let function f be analytic on and inside a closed contour \mathcal{C} enclosing the spectrum of M and H_k , where H_k is an upper Hessenberg matrix generated from the Arnoldi process for M and \mathbf{b} . Then, the error of the Arnoldi iteration for $f(M)\mathbf{b}$ can be expressed as*

$$(3.2) \quad f(M)\mathbf{b} - \text{Arn}_k(f; M, \mathbf{b}) = \left(-\frac{1}{2\pi i} \int_{\mathcal{C}} f(z) \det(h_z(H_k)) h_z(M) dz \right) \boldsymbol{\xi}_0^k.$$

Proof. The result is immediate from [\(3.1\)](#) and [Lemma 3.2](#):

$$\begin{aligned} f(M)\mathbf{b} - \text{Arn}_k(f; M, \mathbf{b}) &= -\frac{1}{2\pi i} \int_{\mathcal{C}} f(z) \boldsymbol{\xi}_z^k dz \\ &= -\frac{1}{2\pi i} \int_{\mathcal{C}} f(z) \det(h_z(H_k)) h_z(M) \boldsymbol{\xi}_0^k dz. \end{aligned} \quad \square$$

Remark 3.4. [Theorem 3.3](#) shows that for any nonsingular M , the error of the Arnoldi iteration for computing $f(M)\mathbf{b}$ is reformulated as the error in solving the linear system $M\mathbf{x} = \mathbf{b}$. This further simplifies the contour integral. For a more general setting, the error admits a bound related to the error of solving shifted linear systems of the form $(M - wI)\mathbf{x} = \mathbf{b}$, where w lies outside the spectrum of both H_k and M ; see Corollary 2.5 in [\[6\]](#) for details.

3.2. Matrix square root. We now turn to deriving an *a priori* error estimate of the Arnoldi process for approximating a matrix square root, that is $f(x) = x^{1/2}$. To ensure the existence of a unique positive definite square root, we assume that M is positive definite. Here, the matrices of interest are non-Hermitian. For such matrices, the eigenvalues may lie off the real axis leading to a contour integral in the complex plane for the error of the Arnoldi process, thereby introducing challenges. We derive the error bound starting from [Theorem 3.3](#), and organize the proof into the following steps:

Step 1: Select an appropriate contour in the complex plane, and derive an initial error bound for the 2-norm of the Arnoldi approximation.

Step 2: Bound the modulus of the complex function $h_z(w)$ using a real-valued function of the modulus, and then estimate $\|h_z(M)\|$ with a new contour integral.

Step 3: Apply the properties of the Beta and Gamma functions to obtain an error bound in terms of the residual \mathbf{r}_0^k for solving $M\mathbf{x} = \mathbf{b}$.

Step 4: Conclude the proof by deriving an upper bound for \mathbf{r}_0^k .
From this, we establish the following theorem.

THEOREM 3.5. *Given a positive-definite matrix $M \in \mathbb{C}^{n \times n}$ and a vector $\mathbf{b} \in \mathbb{C}^n$, the relative error of the Arnoldi process for approximating the matrix square root is*

bounded by

$$\frac{\|M^{1/2}\mathbf{b} - \text{Arn}_k(x^{1/2}; M, \mathbf{b})\|}{\|M^{1/2}\mathbf{b}\|} \leq \frac{2\sqrt{2}(\kappa(M))^{5/2}}{(k-1/2)^{3/4}} \frac{\|\mathbf{r}_0^k\|}{\|\mathbf{b}\|} \leq \frac{4\sqrt{2}(\kappa(M))^{7/2}}{(k-1/2)^{3/4}},$$

where $\kappa(M)$ denotes the condition number of M , defined as $\kappa(M) = \frac{\sigma_{\max}(M)}{\sigma_{\min}(M)}$, and $\sigma_{\max}(M)$ and $\sigma_{\min}(M)$ denote the largest and smallest singular values of M , respectively

Proof. Step 1: Choose an Appropriate Contour. Define \mathcal{C} as a keyhole contour, consisting of a large circular arc \mathcal{C}_R of radius R centered at the origin, a small indented circular arc \mathcal{C}_ϵ of radius ϵ around the origin, and two horizontal line segments \mathcal{C}_δ^+ and \mathcal{C}_δ^- , which run at a small vertical distance $0 < \delta < \epsilon$ above and below the branch cut, respectively (see Figure 1 for details).

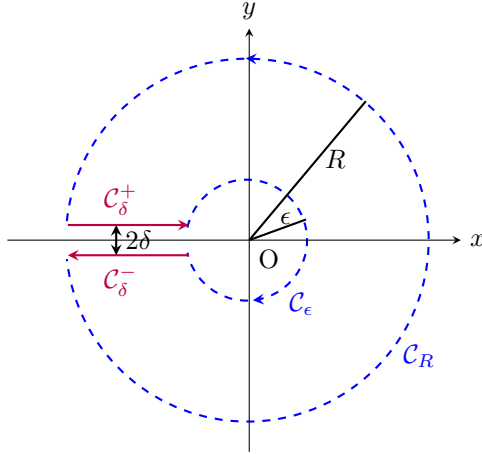


FIG. 1. Keyhole contour with outer circle \mathcal{C}_R , inner circle \mathcal{C}_ϵ , and offset δ above/below the branch cut.

Taking the 2-norm on both sides of (3.2) with $f(z) = z^{1/2}$, we obtain

$$\begin{aligned} \left\| M^{1/2}\mathbf{b} - \text{Arn}_k(f; M, \mathbf{b}) \right\| &\leq \left(\frac{1}{2\pi} \int_{\mathcal{C}_R} |z^{1/2}| \cdot |\det(h_z(H_k))| \cdot \|h_z(M)\| |dz| \right) \|\boldsymbol{\xi}_0^k\| \\ &\quad - \left(\frac{1}{2\pi} \int_{\mathcal{C}_\epsilon} |z^{1/2}| \cdot |\det(h_z(H_k))| \cdot \|h_z(M)\| |dz| \right) \|\boldsymbol{\xi}_0^k\| \\ &\quad + \left(\frac{1}{2\pi} \int_{\mathcal{C}_\delta^+} |z^{1/2}| \cdot |\det(h_z(H_k))| \cdot \|h_z(M)\| |dz| \right) \|\boldsymbol{\xi}_0^k\| \\ &\quad - \left(\frac{1}{2\pi} \int_{\mathcal{C}_\delta^-} |z^{1/2}| \cdot |\det(h_z(H_k))| \cdot \|h_z(M)\| |dz| \right) \|\boldsymbol{\xi}_0^k\|. \end{aligned} \quad (3.3)$$

Let $\mathcal{I}_1, \dots, \mathcal{I}_k \subset \mathbb{C}$ be subsets such that the eigenvalues of H_k are contained in \mathcal{I}_i for $i = 1, \dots, k$. Define the norm $\|h\|_{\mathcal{I}} := \sup_{x \in \mathcal{I}} |h(x)|$ for a function $h(x)$ on $\mathcal{I} \subset \mathbb{C}$, where $|h(x)|$ denotes the modulus of $h(x)$. Note that the Jordan block definition of matrix functions (2.1) implies the eigenvalues of $f(M)$ are exactly $f(\lambda_i)$, where λ_i are

the eigenvalues of M . Thus,

$$|\det(h_z(H_k))| = \left| \prod_{i=1}^k \lambda_i(h_z(H_k)) \right| = \left| \prod_{i=1}^k h_z(\lambda_i(H_k)) \right| \leq \prod_{i=1}^k \|h_z\|_{\mathcal{I}_i}.$$

Plugging this into (3.3) yields

$$\begin{aligned} \left\| M^{1/2} \mathbf{b} - \text{Arn}_k(f; M, \mathbf{b}) \right\| &\leq \left(\frac{1}{2\pi} \int_{\mathcal{C}_R} |z^{1/2}| \cdot \prod_{i=1}^k \|h_z\|_{\mathcal{I}_i} \cdot \|h_z(M)\| |dz| \right) \|\xi_0^k\| \\ &\quad - \left(\frac{1}{2\pi} \int_{\mathcal{C}_\epsilon} |z^{1/2}| \cdot \prod_{i=1}^k \|h_z\|_{\mathcal{I}_i} \cdot \|h_z(M)\| |dz| \right) \|\xi_0^k\| \\ &\quad + \left(\frac{1}{2\pi} \int_{\mathcal{C}_\delta^+} |z^{1/2}| \cdot \prod_{i=1}^k \|h_z\|_{\mathcal{I}_i} \cdot \|h_z(M)\| |dz| \right) \|\xi_0^k\| \\ &\quad - \left(\frac{1}{2\pi} \int_{\mathcal{C}_\delta^-} |z^{1/2}| \cdot \prod_{i=1}^k \|h_z\|_{\mathcal{I}_i} \cdot \|h_z(M)\| |dz| \right) \|\xi_0^k\|. \end{aligned} \quad (3.4)$$

As the outer radius $R \rightarrow \infty$, the integral over the large circular arc vanishes for $k \geq 1$ since $|z^{1/2}| = O(R^{1/2})$, $\|h_z\|_{\mathcal{I}_i} = O(R^{-1})$, and $\|h_z(M)\| = O(R^{-1})$. Similarly, as the inner radius $\epsilon \rightarrow 0$, the integral goes to zero. Thus, as $\epsilon \rightarrow 0$ and $R \rightarrow \infty$, the contributions to the integral come from \mathcal{C}_δ^+ and \mathcal{C}_δ^- . Also, as $\epsilon \rightarrow 0$, δ approaches 0. Then, we have

$$\begin{aligned} &\left\| M^{1/2} \mathbf{b} - \text{Arn}_k(f; M, \mathbf{b}) \right\| \\ &\leq \lim_{\substack{\epsilon \rightarrow 0 \\ R \rightarrow \infty}} \left(\frac{1}{2\pi} \int_{-R}^{-\epsilon} |(x + \delta i)^{1/2}| \cdot \left(\prod_{i=1}^k \|h_{x+\delta i}\|_{\mathcal{I}_i} \right) \cdot \|h_{x+\delta i}(H_k)\| dx \right) \|\xi_0^k\| \\ &\quad - \left(\frac{1}{2\pi} \int_{-\epsilon}^{-R} |(x - \delta i)^{1/2}| \cdot \left(\prod_{i=1}^k \|h_{x-\delta i}\|_{\mathcal{I}_i} \right) \cdot \|h_{x-\delta i}(H_k)\| dx \right) \|\xi_0^k\| \\ &= \left(\frac{1}{\pi} \int_0^\infty x^{1/2} \cdot \left(\prod_{i=1}^k \|h_{-x}\|_{\mathcal{I}_i} \right) \cdot \|h_{-x}(M)\| dx \right) \|\xi_0^k\|. \end{aligned}$$

Step 2: Bound $\|h_{-x}\|_{\mathcal{I}_i}$ and $\|h_{-x}(M)\|$. Consider any $w \in \mathbb{C}$ and a fixed $x \in \mathbb{R}$ such that $x > 0$, then,

$$|w + x| = \sqrt{(\text{Re}(w) + x)^2 + \text{Im}(w)^2} \quad \text{and} \quad \sqrt{|w|^2 + x^2} = \sqrt{\text{Re}(w)^2 + \text{Im}(w)^2 + x^2}.$$

A straightforward calculation then yields

$$|h_{-x}(w)| = \frac{|w|}{|w + x|} \leq \frac{|w|}{\sqrt{|w|^2 + x^2}} := g_x(w).$$

The function $g_x(w)$ is increasing with respect to $|w|$. Noting that $H_k = Q_k^* M Q_k$, we apply the interlacing inequalities for singular values in Theorem 2 of [34] to obtain:

$$\sigma_{\max}(H_k) \leq \sigma_{\max}(M) \quad \text{and} \quad \sigma_{\min}(H_k) \geq \sigma_{\min}(M).$$

Furthermore, the modulus of the eigenvalues of a matrix is bounded above by its largest singular value, and the modulus of the smallest eigenvalue is bounded below by its smallest singular value. Letting $\mathcal{S} := [\sigma_{\min}(M), \sigma_{\max}(M)]$, the problem now turns into analyzing the behavior of g_x within \mathcal{S} ,

$$(3.5) \quad \left\| M^{1/2} \mathbf{b} - \text{Arn}_k(f; M, \mathbf{b}) \right\| \leq \left(\frac{1}{\pi} \int_0^\infty x^{1/2} \cdot \left(\prod_{i=1}^k \|g_x\|_{\mathcal{S}} \right) \cdot \|h_{-x}(M)\| \, dx \right) \|\boldsymbol{\xi}_0^k\|.$$

We next give the bound for $\|h_{-x}(M)\|$. For a fixed real number $x > 0$, we consider a new contour \mathcal{C} as in [Figure 1](#), but with $R = 2\sigma_{\max}(M)$ and $\delta = \frac{\epsilon C_M}{\sqrt{C_M^2 + 4}}$, where

$$C_M = \frac{\lambda_{\min}\left(\frac{M+M^*}{2}\right)}{\left|\lambda_{\min}\left(i\left(\frac{M-M^*}{2}\right)\right)\right|}. \text{ Using the Cauchy integral formula, it follows that}$$

$$h_{-x}(M) = -\frac{1}{2\pi i} \int_{\mathcal{C}} h_{-x}(s)(M - sI)^{-1} \, ds.$$

Then, we have:

$$\begin{aligned} & \|h_{-x}(M)\| \\ & \leq \frac{1}{2\pi} \int_{\mathcal{C}_R} |h_{-x}(s)| \cdot \|(M - sI)^{-1}\| \, |ds| - \frac{1}{2\pi} \int_{\mathcal{C}_\epsilon} |h_{-x}(s)| \cdot \|(M - sI)^{-1}\| \, |ds| \\ & \quad + \frac{1}{2\pi} \int_{\mathcal{C}_\delta^+} |h_{-x}(s)| \cdot \|(M - sI)^{-1}\| \, |ds| - \frac{1}{2\pi} \int_{\mathcal{C}_\delta^-} |h_{-x}(s)| \cdot \|(M - sI)^{-1}\| \, |ds| \\ & \leq \frac{1}{2\pi} \int_{\mathcal{C}_R} |g_x(s)| \cdot \|(M - sI)^{-1}\| \, |ds| - \frac{1}{2\pi} \int_{\mathcal{C}_\epsilon} |g_x(s)| \cdot \|(M - sI)^{-1}\| \, |ds| \\ & \quad + \frac{1}{2\pi} \int_{\mathcal{C}_\delta^+} |g_x(s)| \cdot \|(M - sI)^{-1}\| \, |ds| - \frac{1}{2\pi} \int_{\mathcal{C}_\delta^-} |g_x(s)| \cdot \|(M - sI)^{-1}\| \, |ds|. \end{aligned}$$

Since the integral on the small circular arc tends to 0 as $\epsilon \rightarrow 0$, we only need to take care of the integral along \mathcal{C}_δ^+ , \mathcal{C}_δ^- and over the large circular arc \mathcal{C}_R . On the large circular arc \mathcal{C}_R , we start with the expression:

$$\begin{aligned} \|(M - sI)^{-1}\| &= \frac{1}{\sqrt{\lambda_{\min}((M - sI)^*(M - sI))}} \\ &= \frac{1}{\sqrt{\lambda_{\min}(M^*M - s^*M - sM^* + |s|^2I)}} \\ (3.6) \quad &\leq \frac{1}{\sqrt{\lambda_{\min}(M^*M) + \lambda_{\min}(|s|^2I) + \lambda_{\min}(-s^*M - sM^*)}}. \end{aligned}$$

Letting $T = -s^*M - sM^*$, we get

$$\begin{aligned} \mathbf{x}^* T \mathbf{x} &= -s^* \mathbf{x}^* M \mathbf{x} - s \mathbf{x}^* M^* \mathbf{x} \\ &= -s^* \mathbf{x}^* M \mathbf{x} - s(\mathbf{x}^* M \mathbf{x})^*. \end{aligned}$$

Thus, one obtains $\lambda_{\min}(T) = \min_{\|\mathbf{x}\|=1} \mathbf{x}^* T \mathbf{x} = -2 \max_{\|\mathbf{x}\|=1} \text{Re}(s^* \mathbf{x}^* M \mathbf{x})$. In addition, applying the Cauchy-Schwarz inequality leads to

$$\text{Re}(s^* \mathbf{x}^* M \mathbf{x}) \leq |s^* \mathbf{x}^* M \mathbf{x}| = |s| \cdot |\mathbf{x}^* M \mathbf{x}| \leq |s| \cdot \|M\| = |s| \sigma_{\max}(M).$$

Then, we find $\lambda_{\min}(T) \geq -2|s|\sigma_{\max}(M)$. Substituting the inequality into (3.6), we have

$$\begin{aligned} \|(M - sI)^{-1}\| &\leq \frac{1}{\sqrt{(\sigma_{\min}(M))^2 + |s|^2 - 2|s|\sigma_{\max}(M)}} \\ &= \frac{1}{\sigma_{\min}(M)}. \end{aligned}$$

Thus, over the the large circular arc \mathcal{C}_R , we obtain the following estimate:

$$\begin{aligned} \frac{1}{2\pi} \int_{\mathcal{C}_R} |g_x(s)| \cdot \|(M - sI)^{-1}\| |ds| &\leq \frac{2\pi R}{2\pi\sigma_{\min}(M)} \frac{R}{\sqrt{R^2 + x^2}} \\ &= \frac{4\sigma_{\max}(M)\kappa(M)}{(\sqrt{4(\sigma_{\max}(M))^2 + x^2})}. \end{aligned}$$

Along the lines \mathcal{C}_δ^+ , \mathcal{C}_δ^- , one arrives at

$$\begin{aligned} \|(M - sI)^{-1}\| &= \frac{1}{\sqrt{\lambda_{\min}(M^*M - s^*M - sM^* + |s|^2I)}} \\ (3.7) \quad &\leq \frac{1}{\sqrt{\lambda_{\min}(M^*M) + \lambda_{\min}(-s^*M - sM^*)}}. \end{aligned}$$

Given that M is positive-definite, $\frac{M+M^*}{2}$ is also positive-definite. We assume s takes the form: $s = s_1 \pm i\delta$. Since $\delta = \frac{\epsilon C_M}{\sqrt{C_M^2 + 4}}$ with $C_M = \frac{\lambda_{\min}(\frac{M+M^*}{2})}{|\lambda_{\min}(i(\frac{M-M^*}{2}))|}$, then $-R \leq s_1 \leq -\frac{2\epsilon}{\sqrt{C_M^2 + 4}} < -\epsilon$. Therefore,

$$\begin{aligned} \lambda_{\min}(-s^*M - sM^*) &= -2\lambda_{\max}\left(s_1 \left(\frac{M+M^*}{2}\right) - i\delta \left(\frac{M-M^*}{2}\right)\right) \\ &\geq -2\lambda_{\max}\left(s_1 \left(\frac{M+M^*}{2}\right)\right) - 2\lambda_{\max}\left(-i\delta \left(\frac{M-M^*}{2}\right)\right) \\ &= -2s_1\lambda_{\min}\left(\frac{M+M^*}{2}\right) + 2\delta\lambda_{\min}\left(i \left(\frac{M-M^*}{2}\right)\right) \\ &\geq 0. \end{aligned}$$

Substituting this into (3.7) yields

$$\|(M - sI)^{-1}\| \leq \frac{1}{\sigma_{\min}(M)}.$$

Analogously, with $\delta = \frac{\epsilon C_M}{\sqrt{C_M^2 + 4}}$, we get

$$\begin{aligned}
& \frac{1}{2\pi} \int_{\mathcal{C}_\delta^+} |g_x(s)| \cdot \|(M - sI)^{-1}\| |ds| - \frac{1}{2\pi} \int_{\mathcal{C}_\delta^-} |g_x(s)| \cdot \|(M - sI)^{-1}\| |ds| \\
& \leq \frac{1}{2\pi} \lim_{\epsilon \rightarrow 0} \int_{-R}^{-\epsilon} |g_x(s_1 + \delta i)| \cdot \|(M - (s_1 + \delta i)I)^{-1}\| ds_1 \\
& \quad - \frac{1}{2\pi} \lim_{\epsilon \rightarrow 0} \int_{-\epsilon}^{-R} |g_x(s_1 - \delta i)| \cdot \|(M - (s_1 - \delta i)I)^{-1}\| ds_1 \\
& = \frac{1}{\pi} \int_0^R |g_x(-s_1)| \cdot \|(M + s_1 I)^{-1}\| ds_1 \\
& \leq \frac{R^2}{\pi \sigma_{\min}(M)(\sqrt{R^2 + x^2})} \\
& = \frac{4\sigma_{\max}(M)\kappa(M)}{\pi(\sqrt{4(\sigma_{\max}(M))^2 + x^2})}.
\end{aligned}$$

Finally, combining all estimates, we obtain the upper bound:

$$(3.8) \quad \|h_{-x}(M)\| \leq \frac{1 + \pi}{\pi} \frac{4\sigma_{\max}(M)\kappa(M)}{(\sqrt{4(\sigma_{\max}(M))^2 + x^2})} \leq \frac{4(1 + \pi)\kappa(M)}{\pi} \frac{\sigma_{\max}(M)}{(\sqrt{(\sigma_{\max}(M))^2 + x^2})}.$$

Step 3: Apply Beta and Gamma Functions. Substituting (3.8) into (3.5) gives

$$\begin{aligned}
& \|M^{1/2}\mathbf{b} - \text{Arn}_k(f; M, \mathbf{b})\| \\
& \leq \left(\frac{1}{\pi} \int_0^\infty x^{1/2} \cdot \|g_x(M)\|_S^k \cdot \|h_{-x}\| dx \right) \|\xi_0^k\| \\
& \leq \frac{4(1 + \pi)\kappa(M)}{\pi^2} \left(\int_0^\infty x^{1/2} \cdot \|g_x\|_S^k \cdot \frac{\sigma_{\max}(M)}{(\sqrt{(\sigma_{\max}(M))^2 + x^2})} dx \right) \|\xi_0^k\| \\
& \leq \frac{4(1 + \pi)\kappa(M)}{\pi^2} \left(\int_0^\infty x^{1/2} \cdot \frac{(\sigma_{\max}(M))^{k+1}}{(\sqrt{(\sigma_{\max}(M))^2 + x^2})^{k+1}} dx \right) \|\xi_0^k\|.
\end{aligned}$$

Define $\mathbf{I} := \int_0^\infty x^{1/2} \cdot \frac{(\sigma_{\max}(M))^{k+1}}{(\sqrt{(\sigma_{\max}(M))^2 + x^2})^{k+1}} dx$. Let $x = \sigma_{\max}(M)y$, then we obtain

$$\begin{aligned}
\mathbf{I} & = (\sigma_{\max}(M))^{3/2} \int_0^\infty \frac{y^{1/2}}{(\sqrt{1 + y^2})^{k+1}} dy \\
& = (\sigma_{\max}(M))^{3/2} \int_0^{\pi/2} \frac{(\tan(\theta))^{1/2} (\sec(\theta))^2}{(\sec(\theta))^{k+1}} d\theta \\
& = (\sigma_{\max}(M))^{3/2} \int_0^{\pi/2} (\sin(\theta))^{1/2} (\cos(\theta))^{k-3/2} d\theta \\
& = \frac{(\sigma_{\max}(M))^{3/2}}{2} \text{B}\left(\frac{3}{4}, \frac{k}{2} - \frac{1}{4}\right) \\
& = \frac{(\sigma_{\max}(M))^{3/2}}{2} \frac{\Gamma(3/4)\Gamma(k/2 - 1/4)}{\Gamma(k/2 + 1/2)}.
\end{aligned}$$

Here, $B(\cdot, \cdot)$ and $\Gamma(\cdot)$ are the standard Beta and Gamma functions, respectively, with $B(x, y) = \frac{\Gamma(x)\Gamma(y)}{\Gamma(x+y)}$. Furthermore, noting that in [36] for $w > 0$ and $l \in (0, 1)$,

$$\left(\frac{w}{w+l}\right)^{1-l} \leq \frac{\Gamma(w+l)}{w^l \Gamma(w)} \leq 1,$$

we arrive at

$$\begin{aligned} \frac{\Gamma(k/2 - 1/4)}{\Gamma(k/2 + 1/2)} &\leq \frac{(k/2 + 1/2)^{1/4}}{(k/2 - 1/4)^{1/4}(k/2 - 1/4)^{3/4}} \\ &\leq \frac{2^{5/4}}{(k - 1/2)^{3/4}} \\ &\leq \frac{\sqrt{2}\pi^2}{(1 + \pi)\Gamma(3/4)(k - 1/2)^{3/4}}. \end{aligned}$$

Then, it holds that

$$I \leq \frac{\pi^2(\sigma_{\max}(M))^{3/2}}{\sqrt{2}(1 + \pi)(k - 1/2)^{3/4}}.$$

Collecting all estimates leads to

$$\|M^{1/2}\mathbf{b} - \text{Arn}_k(f; M, \mathbf{b})\| \leq \frac{2\sqrt{2}\kappa(M)(\sigma_{\max}(M))^{3/2}}{(k - 1/2)^{3/4}} \|\boldsymbol{\xi}_0^k\|.$$

Thus, the relative error of the Arnoldi approximation for matrix square roots is bounded by:

$$\begin{aligned} \frac{\|M^{1/2}\mathbf{b} - \text{Arn}_k(x^{1/2}; M, \mathbf{b})\|}{\|M^{1/2}\mathbf{b}\|} &\leq \frac{2\sqrt{2}\kappa(M)(\sigma_{\max}(M))^{3/2}}{(k - 1/2)^{3/4}} \frac{\|\boldsymbol{\xi}_0^k\|}{\|M^{1/2}\mathbf{b}\|} \\ (3.9) \quad &\leq \frac{2\sqrt{2}(\kappa(M))^{5/2}}{(k - 1/2)^{3/4}} \frac{\|\mathbf{r}_0^k\|}{\|\mathbf{b}\|}. \end{aligned}$$

Step 4: Bound $\|\mathbf{r}_0^k\|$. From (2.2), it holds that

$$\begin{aligned} \mathbf{r}_0^k &= \mathbf{b} - MQ_k H_k^{-1} \|\mathbf{b}\| \mathbf{e}_1 \\ &= \mathbf{b} - (Q_k H_k + h_{k+1,k} \mathbf{q}_{k+1} \mathbf{e}_k^T) H_k^{-1} \|\mathbf{b}\| \mathbf{e}_1 \\ &= -h_{k+1,k} \mathbf{q}_{k+1} \mathbf{e}_k^T H_k^{-1} \|\mathbf{b}\| \mathbf{e}_1. \end{aligned}$$

Taking the 2-norm on both sides gives

$$(3.10) \quad \|\mathbf{r}_0^k\| \leq h_{k+1,k} \|H_k^{-1}\| \|\mathbf{b}\| \leq \frac{h_{k+1,k}}{\sigma_{\min}(H_k)} \|\mathbf{b}\|.$$

Multiplying \mathbf{e}_k on both sides of (2.2) and then taking the 2-norm, we have

$$(3.11) \quad h_{k+1,k} = \|M\mathbf{q}_k - Q_k H_k \mathbf{e}_k\| \leq \|M\mathbf{q}_k\| + \|H_k \mathbf{e}_k\| \leq \sigma_{\max}(M) + \sigma_{\max}(H_k),$$

where the second inequality is achieved by utilizing the triangle inequality and the orthogonality of Q_k . Plugging the above estimate into (3.10) and utilizing the interlacing inequalities for singular values, we further bound $\|\mathbf{r}_0^k\|$ by

$$\|\mathbf{r}_0^k\| \leq \frac{\sigma_{\max}(M) + \sigma_{\max}(H_k)}{\sigma_{\min}(H_k)} \|\mathbf{b}\| \leq \frac{2\sigma_{\max}(M)}{\sigma_{\min}(M)} \|\mathbf{b}\| = 2\kappa(M) \|\mathbf{b}\|.$$

Consequently, substituting the above estimate of \mathbf{r}_0^k into (3.9), we obtain

$$\frac{\|M^{1/2}\mathbf{b} - \text{Arn}_k(x^{1/2}; M, \mathbf{b})\|}{\|M^{1/2}\mathbf{b}\|} \leq \frac{2\sqrt{2}(\kappa(M))^{5/2}}{(k-1/2)^{3/4}} \frac{\|\mathbf{r}_0^k\|}{\|\mathbf{b}\|} \leq \frac{4\sqrt{2}(\kappa(M))^{7/2}}{(k-1/2)^{3/4}}. \quad \square$$

Remark 3.6. If the matrix M is Hermitian, then using the results from [6] and [1], we obtain

$$\frac{\|M^{1/2}\mathbf{b} - \text{Arn}_k(x^{1/2}; M, \mathbf{b})\|}{\|M^{1/2}\mathbf{b}\|} \leq \frac{(\kappa(M))^{3/2}}{2k^{3/2}} \frac{\|\mathbf{r}_0^k\|}{\|\mathbf{b}\|} \leq \frac{(\kappa(M))^{5/2}}{k^{3/2}}.$$

This sharper result stems from the fact that the Hermitian matrix is unitarily diagonalizable with real eigenvalues, which allows for a more refined spectral analysis of $|\det(h_z(H_k))|$ and $\|h_z(M)\|$ in (3.3).

Remark 3.7. Note that the residual \mathbf{r}_0^k is precisely the residual from the FOM applied to the linear system $M\mathbf{x} = \mathbf{b}$. Since the error in Theorem 3.5 is bounded in terms of \mathbf{r}_0^k , which is naturally computed in the Arnoldi iteration, we thus have a practical stopping criterion for our algorithm.

Remark 3.8. The bound in (3.11) is a loose upper bound for $h_{k+1,k}$. In practice, $h_{k+1,k}$ tends to decrease with k , as the Krylov subspace increasingly approximates the spectral subspace associated with the dominant eigenvalues of M . However, this behavior is not guaranteed in general. To further understand the behavior of $\|\mathbf{r}_0^k\|$, one may explore results from [7]. They show that $\min_{0 \leq j \leq k} \|\mathbf{r}_0^j\| \leq \sqrt{k+1} \cdot \|\mathbf{r}_G^k\|$, where \mathbf{r}_G^k denotes the GMRES residual after k iterations for solving $M\mathbf{x} = \mathbf{b}$. This implies that the overall convergence of FOM is at most a factor of $\sqrt{k+1}$ worse than that of GMRES. However, the residual norm at a fixed iteration k can be arbitrarily large, and thus this result does not apply to our setting.

3.3. Preprocessing. In practice, matrices arising from large-scale problems are often too large to be directly measured, stored, or analyzed, necessitating efficient preprocessing. To further reduce the cost, one direction is to employ data-sparse approximations, such as hierarchical or low-rank representations [5, 8, 10, 17, 22, 23]. These methods accelerate matrix-vector multiplications by compressing the underlying structure of the matrix. Under this framework, we modify the results from Theorem 3.5 to get an error bound for approximating the square root of a preprocessed matrix using the Arnoldi iteration. This is summarized in the following theorem.

THEOREM 3.9. *Given a positive-definite matrix $M \in \mathbb{C}^{n \times n}$ and a vector $\mathbf{b} \in \mathbb{C}^n$, assume that M admits a data-sparse approximation \widetilde{M} which is positive definite and satisfies, for some $0 < \epsilon < 1/\kappa(M)$, $\|M - \widetilde{M}\|_* \leq \epsilon\|M\|$. Then, the relative error of the Arnoldi process for approximating the matrix square root is bounded by*

$$\frac{\|M^{1/2}\mathbf{b} - \text{Arn}_k(x^{1/2}; \widetilde{M}, \mathbf{b})\|}{\|M^{1/2}\mathbf{b}\|} \leq \epsilon^{1/2}\kappa^{1/2}(M) + \frac{4\sqrt{2}(1+\epsilon)^{7/2}(\kappa(M))^{9/2}}{(k-1/2)^{3/4}(1-\epsilon\kappa(M))^{9/2}}.$$

Proof. Based on \widetilde{M} , we apply the Arnoldi process to compute the matrix square root. Now the problem turns into:

$$\frac{\|M^{1/2}\mathbf{b} - \text{Arn}_k(x^{1/2}; \widetilde{M}, \mathbf{b})\|}{\|M^{1/2}\mathbf{b}\|} \leq \frac{\|M^{1/2}\mathbf{b} - \widetilde{M}^{1/2}\mathbf{b}\|}{\|M^{1/2}\mathbf{b}\|} + \frac{\|\widetilde{M}^{1/2}\mathbf{b} - \text{Arn}_k(x^{1/2}; \widetilde{M}, \mathbf{b})\|}{\|M^{1/2}\mathbf{b}\|}.$$

For the first term on the right hand side, according to the Powers–Størmer inequality [32], we have

$$\frac{\|M^{1/2}\mathbf{b} - \widetilde{M}^{1/2}\mathbf{b}\|}{\|M^{1/2}\mathbf{b}\|} \leq \frac{\|M^{1/2} - \widetilde{M}^{1/2}\| \|\mathbf{b}\|}{\|M^{1/2}\mathbf{b}\|} \leq \frac{\|M - \widetilde{M}\|_*^{1/2} \|\mathbf{b}\|}{\|M^{1/2}\mathbf{b}\|} \leq \epsilon^{1/2} \kappa^{1/2}(M).$$

With Theorem 3.5, the second term is bounded by:

$$\frac{\|\widetilde{M}^{1/2}\mathbf{b} - \text{Arn}_k(x^{1/2}; \widetilde{M}, \mathbf{b})\|}{\|\widetilde{M}^{1/2}\mathbf{b}\|} \leq \frac{4\sqrt{2}(\kappa(\widetilde{M}))^{7/2}}{(k-1/2)^{3/4}}.$$

By Weyl's inequality [4], we have $|\sigma_k(M) - \sigma_k(\widetilde{M})| \leq \|M - \widetilde{M}\| \leq \|M - \widetilde{M}\|_* \leq \epsilon \|M\| = \epsilon \sigma_{\max}(M)$. Rearranging terms gives

$$\kappa(\widetilde{M}) \leq \frac{(1+\epsilon)\sigma_{\max}(M)}{\sigma_{\min}(M) - \epsilon\sigma_{\max}(M)} = \frac{(1+\epsilon)\kappa(M)}{1 - \epsilon\kappa(M)}.$$

Therefore, we conclude that

$$\begin{aligned} \frac{\|\widetilde{M}^{1/2}\mathbf{b} - \text{Arn}_k(x^{1/2}; \widetilde{M}, \mathbf{b})\|}{\|M^{1/2}\mathbf{b}\|} &\leq \frac{4\sqrt{2}(\kappa(\widetilde{M}))^{7/2}}{(k-1/2)^{3/4}} \frac{\|M^{1/2}\mathbf{b}\|}{\|\widetilde{M}^{1/2}\mathbf{b}\|} \\ &\leq \frac{4\sqrt{2}(1+\epsilon)^{7/2}(\kappa(\widetilde{M}))^{9/2}}{(k-1/2)^{3/4}(1 - \epsilon\kappa(M))^{9/2}}. \quad \square \end{aligned}$$

4. Numerical experiments and discussion. In this section, we report on numerical studies of the Arnoldi iteration for computing the matrix square root applied to a vector, that is, $M^{1/2}\mathbf{b}$. First, we explore various matrix settings to study the dependence of relative error on the condition number of matrices and the iteration count. We start with a Hermitian matrix, confirming the result in Remark 3.6 as well as Lemma 3.3 in [1]. Then, we test both sparse and general non-Hermitian matrices validating Theorem 3.5. Finally, we explore the use of the Arnoldi iteration for computing $M^{1/2}\mathbf{b}$ in the simulation of particulate suspensions to demonstrate the effectiveness of the proposed method in practical applications. Consistently across examples, the Arnoldi approximation is terminated based on the relative residual norm for solving $M\mathbf{x} = \mathbf{b}$, with a tolerance of 10^{-2} . In particular, all residuals and relative errors reported in this section are measured in the 2-norm.

4.1. 2D Laplacian. In this example, we consider the SPD matrix M arising from a five-point stencil discretization of the Laplace equation with homogeneous Dirichlet boundary conditions on the unit square domain. The discrete problem is formulated on a uniform numerical grid with grid spacing $h = \frac{1}{n}$, where n denotes the number of divisions along each axis. Then, M takes the form of a block-structured matrix:

$$M := \begin{pmatrix} C & D & 0 & \cdots & 0 \\ D & C & D & \cdots & 0 \\ 0 & D & C & \cdots & 0 \\ \vdots & \vdots & \vdots & \ddots & \vdots \\ 0 & 0 & 0 & D & C \end{pmatrix}$$

where, C and D are defined as:

$$C = \text{tridiag} \left(-\frac{1}{h^2}, \frac{4}{h^2}, -\frac{1}{h^2} \right)_{(n-1) \times (n-1)},$$

$$D = \text{diag} \left(-\frac{1}{h^2}, -\frac{1}{h^2}, \dots, -\frac{1}{h^2} \right)_{(n-1) \times (n-1)}.$$

In this case, vector \mathbf{b} is taken to be the vector of all ones. The performance of the Arnoldi iteration for computing $M^{1/2}\mathbf{b}$ is presented in Table 1. The numerical experiments confirm that as the condition number of the matrix increases, maintaining a relative error on the order of 10^{-5} requires a larger number of iterations. The decay of the normalized residual for FOM and the relative error for the Arnoldi method are depicted in Figure 2. In this example, a normalized residual of 10^{-2} for FOM yields a relative error of approximately 10^{-5} in the Arnoldi approximation, showing a three order of magnitude improvement. This observation indicates that employing the normalized residual of FOM as a stopping criterion is both effective and efficient, enabling accurate results even with a relatively large tolerance. To gain further insight into this example, we study the relationship between the relative error, condition number, and iteration count. The log-log plot of the relative error decay against the iteration count k for different condition numbers is shown in Figure 3. We observe that the error exhibits a decay rate of approximately $\mathcal{O}(k^{-3/2})$ with respect to the iteration count k . Additionally, we fix $k = 25$ and plot the relative error against the condition number on a log-log scale in Figure 4. As shown, the error decay scales with the condition number κ at a rate close to $\mathcal{O}(\kappa^{5/2})$. These results are consistent with the conclusions for Hermitian matrices stated in Remark 3.6 and Lemma 3.3 in [1].

TABLE 1

Condition number of M , iteration counts, and relative error of the Arnoldi iteration for the discrete 2D Laplacian.

n	$\kappa(M)$	Relative Error	Iteration Counts k
30	529.97	1.90e-05	29
40	942.53	1.59e-05	39
50	1472.96	1.07e-05	50
60	2121.27	9.98e-06	60
70	2887.45	7.84e-06	71
80	3771.51	7.57e-06	81
90	4773.44	6.31e-06	92
100	5893.24	6.22e-06	102
110	7130.92	4.69e-06	114

4.2. Convection-Diffusion problem. In this case, M is taken from the discretization of the convection-diffusion problem, which describes transport phenomena in a given domain. The continuous convection-diffusion operator is defined as

$$Lu := \eta u''(x) + u'(x), \quad x \in [0, 1],$$

subject to homogeneous Dirichlet boundary conditions. Here, η is the diffusion coefficient. For small values of η , the problem is convection-dominated. To accurately

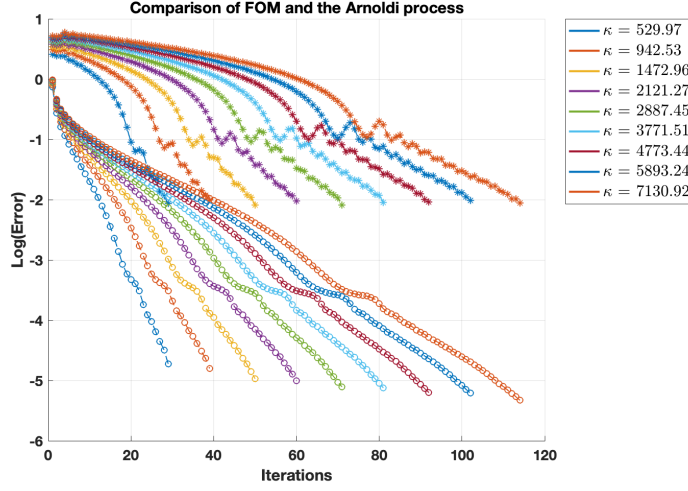


FIG. 2. Semi-log plot of the normalized residual for FOM (*) and the relative error for Arnoldi (o-) with different condition number against iteration count k for the discrete 2D Laplacian.

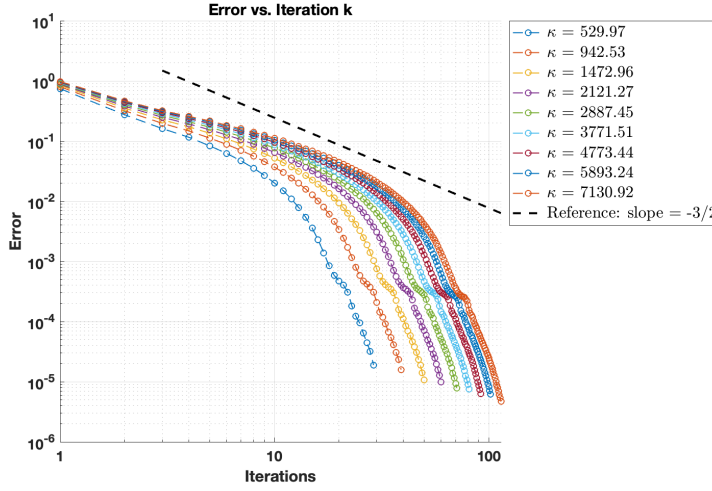


FIG. 3. Log-log plot of relative error decay with varying condition numbers against iteration count k for the discrete 2D Laplacian.

capture the convection effects while maintaining numerical stability, we employ an up-wind scheme. A uniform numerical grid with grid spacing $h = \frac{1}{n}$ is adopted, where the discrete points are defined as $x_i = ih$, $i = 0, 1, 2, \dots, n$. The resulting finite-difference scheme of the operator takes the following form:

$$\eta \frac{u_{i+1} - 2u_i + u_{i-1}}{h^2} + \frac{u_i - u_{i-1}}{h},$$

where u_i represents the numerical approximation to $u(x_i)$. Let M be the tridiagonal matrix obtained from the above finite-difference discretization of L . We take \mathbf{b} to be the vector with all entries equal to one, and fix $\eta = 0.1$.

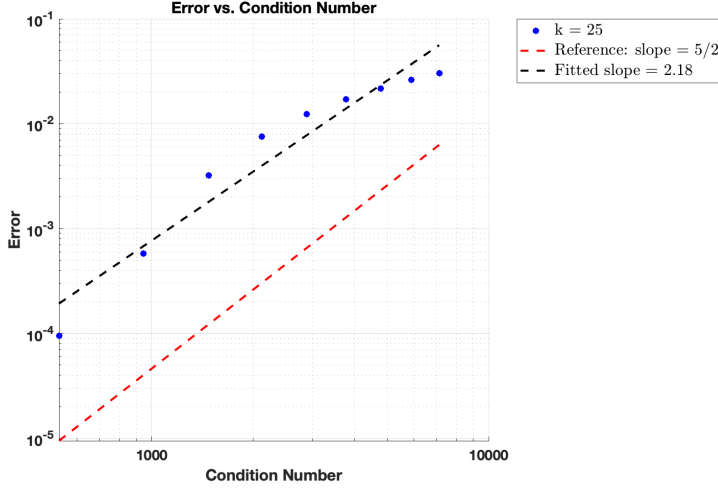


FIG. 4. Log-log plot of relative error with $k = 25$ against condition number for the discrete 2D Laplacian.

The results for approximating $M^{1/2}\mathbf{b}$ are summarized in Table 2 and Figure 5, and the general trends align with the conclusions drawn from the 2D Laplacian example. However, the matrix in this case is no longer symmetric. From the plot of the error versus iteration count in Figure 6, we see that as the condition number increases, the convergence rate closely follows a $k^{-3/4}$ relationship with respect to the iteration count. This observation is consistent with the theoretical result established in Theorem 3.5. Meanwhile, for a fixed $k = 480$, Figure 6 indicates that for large condition numbers, the observed trend closely follows $\kappa^{7/2}$.

TABLE 2
Condition number of M , iteration counts, and relative error of the Arnoldi iteration for the convection-diffusion problem.

n	$\kappa(M)$	Relative Error	Iteration Counts k
500	67510.90	3.99e-08	495
600	97087.72	3.31e-08	594
700	132022.80	2.85e-08	693
800	172316.14	2.53e-08	792
900	217967.73	2.29e-08	891
1000	268977.57	2.10e-08	990
1100	325345.68	1.94e-08	1089
1200	387072.03	1.81e-08	1188
1300	454156.65	1.71e-08	1287

4.3. General matrices. Next, we consider positive definite but non-symmetric dense matrices. The matrix M is constructed as follows:

$$(4.1) \quad M = M_0 + \alpha I = USV^T + \alpha I,$$

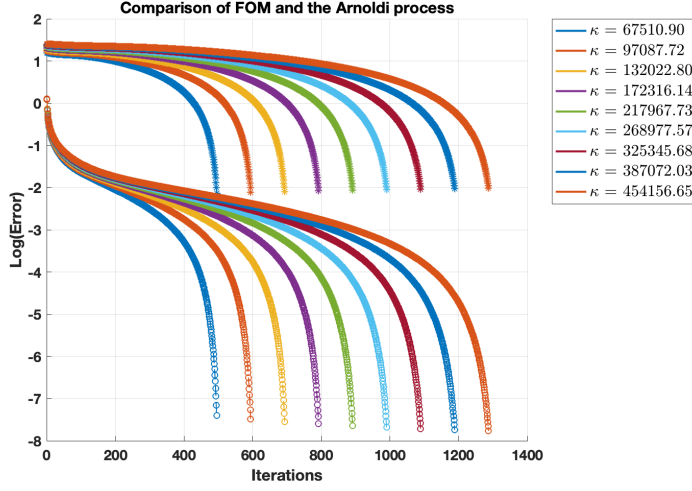


FIG. 5. Semi-log plot of the normalized residual for FOM (*-) and the relative error for Arnoldi (o-) with different condition number against iteration count k for the convection-diffusion problem.

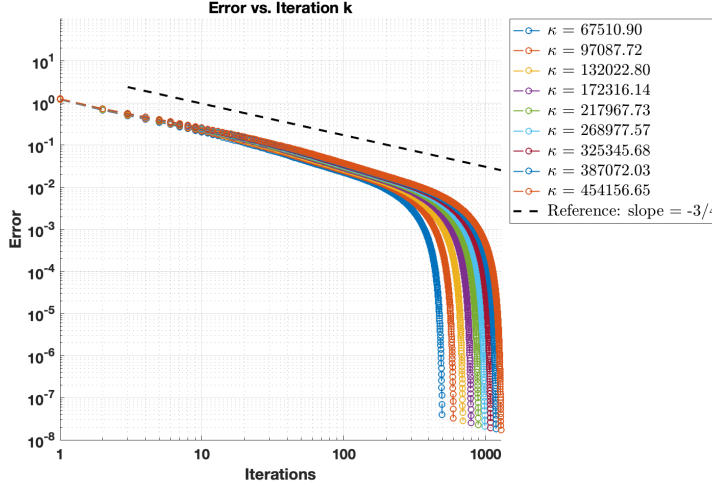


FIG. 6. Log-log plot of relative error decay with varying condition numbers against iteration count k for the convection-diffusion problem.

where M_0 is a low-rank matrix with rank m , U and V are orthonormal matrices generated randomly, and S is an $m \times m$ diagonal matrix whose entries decay logarithmically from 1 to $\frac{1}{\beta}$, where β is a given constant. A shift term, αI , is introduced to ensure positive-definiteness of M . Specifically, the shift parameter α is defined as: $\alpha = -(1 + 5 \times 10^{-3}) \min \operatorname{Re}(\lambda_{\min}(M_0))$. As a result, the condition number of the M is influenced by both α and β . In this test, we set the rank to $m = 500$, and the size of the matrix M is 5000×5000 . The parameter β takes values of 400, 600, 800, 1000, 1200, 1400, 1600, 1800, 2000. As before, \mathbf{b} is taken to be the vector of all ones.

In Table 3, we display the corresponding results. As the relative error remains

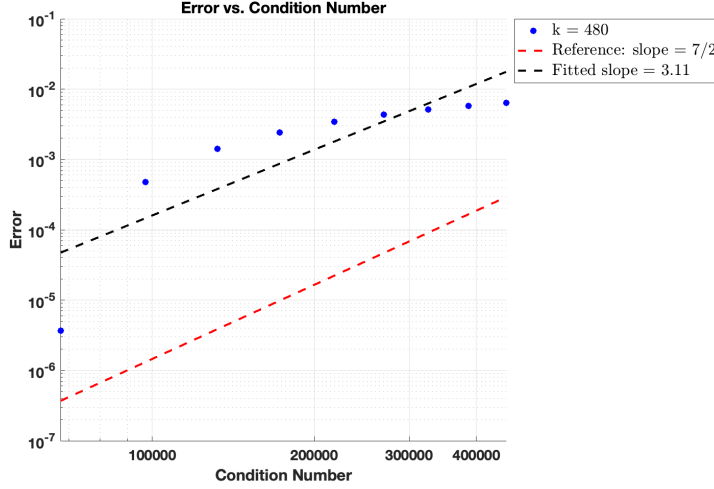


FIG. 7. Log-log plot of relative error with $k = 480$ against condition number for the convection-diffusion problem.

around 10^{-5} , the number of iterations generally increases with the condition number. Similarly, the normalized residual for solving $M\mathbf{x} = \mathbf{b}$ provides an effective stopping criterion for the Arnoldi iteration in the evaluation of $M^{1/2}\mathbf{b}$ (Figure 8). As seen in Figure 9, the error decay of the Arnoldi method closely follows the reference slope before the transition to superlinear convergence. However, we observe that with the iteration count fixed at $k = 35$, the fitted slope is approximately 0.9, which is much smaller than the theoretical value of $7/2$. These observations indicate that the theoretical results established in Theorem 3.9 yield a reasonably tight estimate for the iteration count k , but only a loose upper bound with respect to the condition number for certain type of matrices. This may be due to the fact that the bounds could depend not only on the condition number and iteration counts but also on intrinsic spectral characteristics or a specific structure of the matrices.

TABLE 3

Condition number of M , iteration counts, and relative error of the Arnoldi iteration for general matrices constructed via (4.1).

$\kappa(M)$	Relative Error	Iteration Counts k
2192.38	2.40e-05	38
5375.35	2.90e-05	41
9325.42	2.62e-05	56
28826.11	3.86e-05	38
32437.66	2.45e-05	47
47395.74	2.87e-05	58
52845.93	6.31e-05	36
166131.16	5.27e-05	63
188372.52	1.03e-04	51

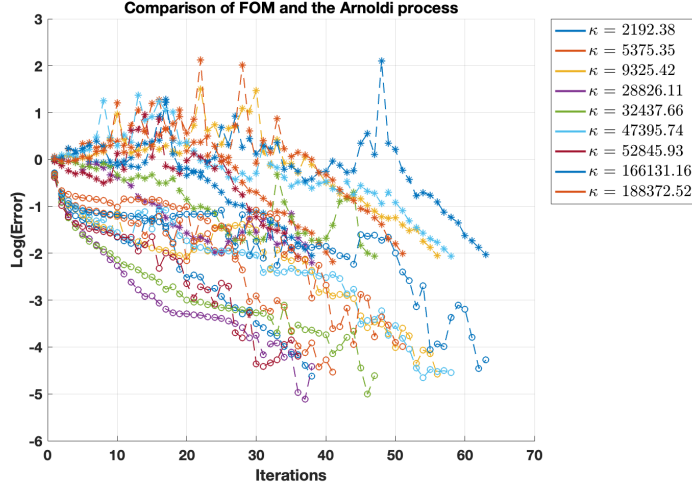


FIG. 8. Semi-log plot of the normalized residual for FOM (*-) and the relative error for Arnoldi (o-) with different condition number against iteration count k for general matrices constructed via (4.1).

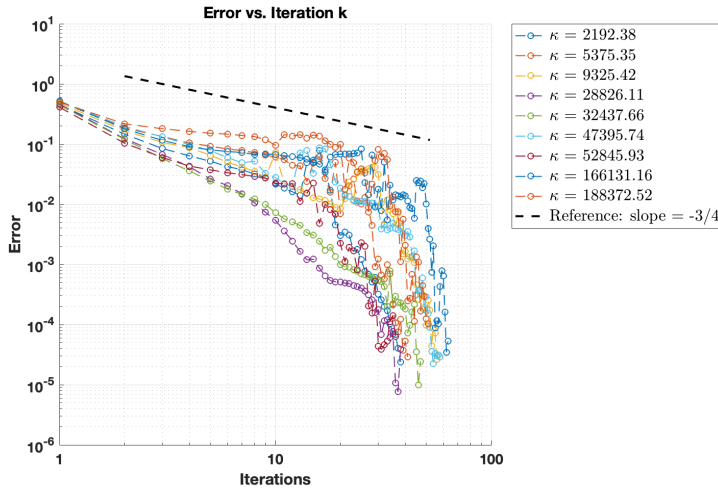


FIG. 9. Log-log plot of relative error decay with varying condition numbers against iteration count k for general matrices constructed via (4.1).

4.4. Practical application. The study of particulate suspensions is of great interest, and plays critical roles in diverse fields such as materials design [27], biological systems [27], micro-robotics [37], and food processing [21]. Immersed in a fluid environment, particles' mobility is dictated by the hydrodynamic interactions between the particles. At micro scales, particles are also subject to thermal fluctuations, in the form of Brownian motion. The configuration of particles evolves over time and is governed by the overdamped limit of Langevin dynamics [14]. Thus, the computation of particles' Brownian displacements crucially rely on the mobility matrix, and

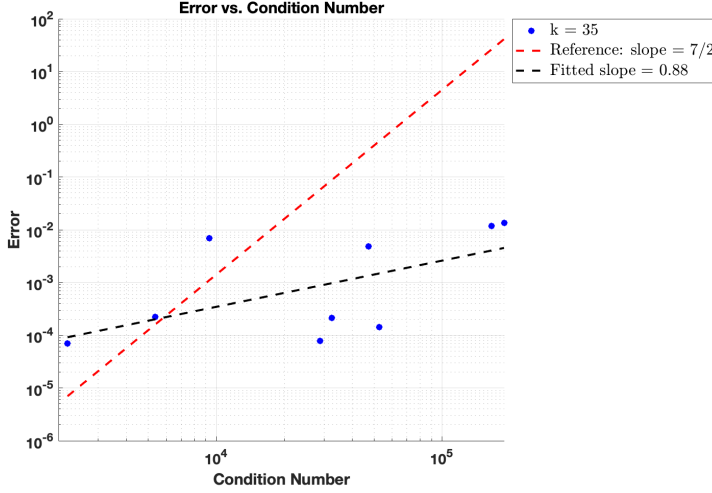


FIG. 10. Log-log plot of relative error with $k = 35$ against condition number for general matrices constructed via (4.1).

its square root, both dependent on all particles' instantaneous positions. Efficiently computing these two matrices remains a significant computational challenge.

Since hydrodynamic interactions depend on the separation distance between particles, the particle interactions weaken as the distance increases [25]. As a result, far-field blocks in the mobility matrix exhibit low-rank structure, and can then be efficiently approximated. To this end, the Hydrodynamic Interaction Graph Neural Network (HIGNN) framework, proposed in [25, 24], maps the many-body hydrodynamic interactions onto a graph neural network. By employing hierarchical-matrices using adaptive cross approximation [17], the computational complexity for using HIGNN to compute particles' velocities given any applied forces can be reduced to nearly linear [26].

In the following tests, M is the mobility matrix obtained from the HIGNN model and has been preprocessed into a hierarchical-matrix form. Also, we assume that a uniform gravitational force \mathbf{b} is applied to each particle. This numerical example focuses on evaluating the effectiveness of the Arnoldi iteration on computing $M^{1/2}$ in a long-time dynamic simulation of particles' sedimentation. In the simulations, the explicit Euler method was adopted as the temporal integrator to update particles' positions from their velocities, with a time step of $\Delta t = 0.005$. At each time step, the HIGNN is applied to predict the velocities of all particles. To generate the initial cubic-lattice like configuration of particles, the particles are first positioned at grid points with a spacing of 4, and then each particle is randomly perturbed with a displacement of magnitude 0.2 from its original position. With this initial configuration, we simulate particles sedimenting in an unbounded domain. The number of particles, N , considered here varies from 20^3 to 100^3 . For such large systems, direct computation of the square root of the mobility matrix M can be computationally expensive. To address this and evaluate the accuracy of the Arnoldi iteration in this context, we apply the Arnoldi process twice to approximate $M\mathbf{b} = M^{1/2}(M^{1/2}\mathbf{b})$. Thus, the relative error is defined as $\frac{\|M\mathbf{b} - \text{Arn}_k(x^{1/2}; M, \text{Arn}_k(x^{1/2}; M, \mathbf{b}))\|}{\|M\mathbf{b}\|}$.

The snapshots at the 1st, 100th, and 200th time steps from the simulation of a

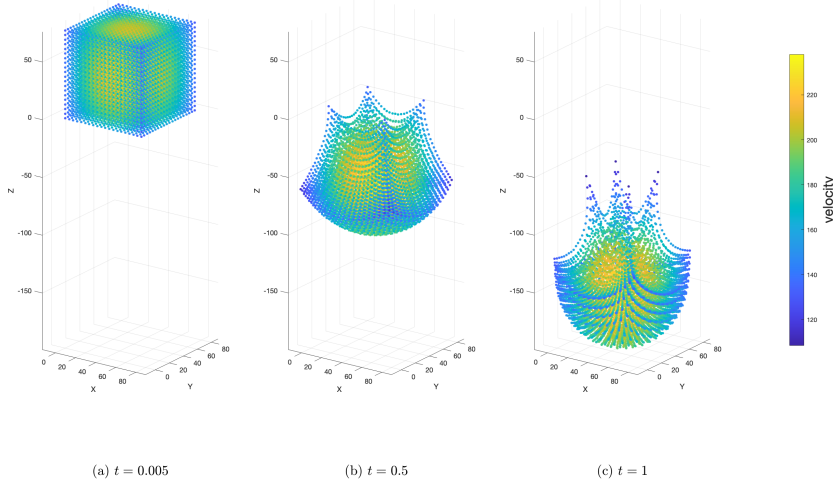


FIG. 11. Snapshots of 8000 particles sedimenting in an unbounded domain at times $t = 0.005$, 0.25, and 1, respectively, simulated using the HIGNN. The color is correlated to the particles' velocity magnitude.

TABLE 4
Arnoldi Approximation for lattice structure system with constant particle concentration.

N	Iteration Counts k	Relative Error
20^3	10	2.06699e-04
40^3	14	1.34295e-04
60^3	15	1.70283e-04
80^3	18	3.11680e-04
100^3	21	3.86345e-04

20^3 particle system are presented in Figure 11. Letting M be the mobility matrix at the 100th time step, Table 4 records the number of iterations k required to compute $M^{1/2}\mathbf{b}$ and the relative error as the number of particles N increases from 20^3 to 100^3 . Note that in this scenario, since the initial spacing between particles is kept the same as N increases, a consistent particle concentration is maintained. One sees that as the number of particles increases, the number of iterations required to compute the matrix square root applied to a vector remains relatively low and does not grow significantly, while maintaining a relative error on the order of 10^{-4} . This is because the matrix is well conditioned. Furthermore, we depict the relationship between the number of particles and the runtime on a log-log scale in Figure 12. The plot implies that the Arnoldi approximation, based on the hierarchical matrix representation, exhibits an $O(N \log N)$ time complexity.

Next, we consider 40^3 particles arranged in a similar initial cubic lattice as above, but with the grid spacing d varying from 3 to 5 (still perturbed by a displacement of 0.2). With this change, we consider different particle concentrations; when d in-

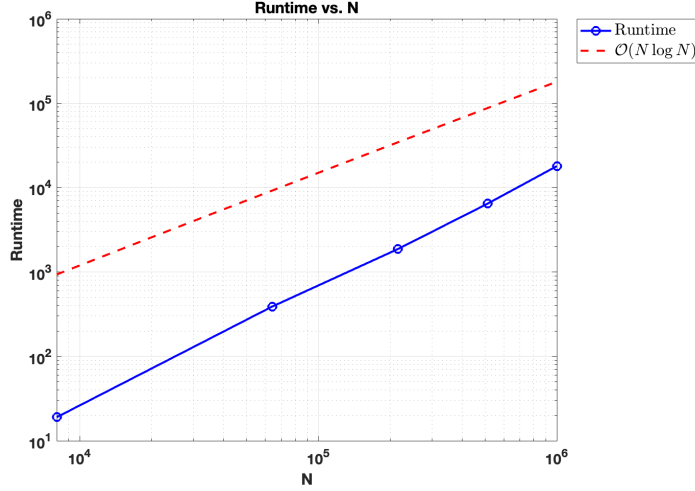


FIG. 12. Log-log plot of runtime against number of particles for lattice structure system.

creases, the particle concentration decreases, thus lowering the required rank of the approximation to the corresponding blocks. As shown in Table 5, lower particle concentration leads to reduced runtime for the Arnoldi approximation. However, the required number of iterations remains relatively small and stable compared to the matrix size. In this test, M corresponds to the mobility matrix attained at the 50th time step.

TABLE 5
Arnoldi Approximation for lattice structure with different particle concentration.

d	Iteration Counts k	relative error	runtime
3	12	1.93793e-04	362.4649
3.5	12	1.81240e-04	386.0504
4	10	1.88017e-04	319.9872
4.5	10	1.86118e-04	307.9138
5	10	1.83476e-04	298.9904

5. Concluding remarks. In this work, we derive *a priori* error estimates of the Arnoldi process for approximating the matrix square root applied to a vector, extending the results in [6] for Hermitian matrices to non-Hermitian cases. Moreover, we provide an error bound based on a data-sparse representation of the matrix. Through numerical experiments, we investigate the convergence behavior of the Arnoldi iteration for computing $M^{1/2}\mathbf{b}$ across different matrix types. The observations indicate that the theoretical results presented in Theorem 3.5 appear to be sharp in terms of iteration count, yet remain a loose upper bound with respect to the condition number for certain classes of matrices. Additionally, we consider the mobility matrix arising from particulate suspension simulations, where the matrix is approximated into a hierarchical matrix. The numerical results demonstrate the effectiveness of our approach for large-scale problems. Future extensions of this paper include deriving a sharper dependence on the condition number for approximating the matrix square root ap-

plied to a vector via Arnoldi iteration, as well as investigating the error behavior of GMRES in the approximation of $f(M)\mathbf{b}$ for general functions f .

Acknowledgments. The authors would like to thank Zhan Ma and Zisheng Ye for their valuable discussions and assistance with the code implementation. The authors also gratefully acknowledge support from the National Science Foundation under Grant No. DMS-2208267 and the Army Research Office under Grant No. W911NF2310256.

REFERENCES

- [1] N. AMSEL, T. CHEN, A. GREENBAUM, C. MUSCO, AND C. MUSCO, *Near-optimal approximation of matrix functions by the lanczos method*, arXiv preprint arXiv:2303.03358, (2023).
- [2] R. M. ASL, Y. S. HAGH, S. SIMANI, H. HANDROOS, ET AL., *Adaptive square-root unscented kalman filter: An experimental study of hydraulic actuator state estimation*, Mechanical Systems and Signal Processing, 132 (2019), pp. 670–691.
- [3] J. M. BARDSLEY, *Mcmc-based image reconstruction with uncertainty quantification*, SIAM Journal on Scientific Computing, 34 (2012), pp. A1316–A1332.
- [4] R. BHATIA, *Matrix Analysis*, Springer, New York, 1997.
- [5] E. K. BJARKASON, *Pass-efficient randomized algorithms for low-rank matrix approximation using any number of views*, SIAM Journal on Scientific Computing, 41 (2019), pp. A2355–A2383.
- [6] T. CHEN, A. GREENBAUM, C. MUSCO, AND C. MUSCO, *Error bounds for lanczos-based matrix function approximation*, SIAM Journal on Matrix Analysis and Applications, 43 (2022), pp. 787–811.
- [7] T. CHEN AND G. MEURANT, *Near-optimal convergence of the full orthogonalization method*, arXiv preprint arXiv:2403.07259, (2024).
- [8] K. L. CLARKSON AND D. P. WOODRUFF, *Low-rank approximation and regression in input sparsity time*, Journal of the ACM (JACM), 63 (2017), pp. 1–45.
- [9] A. CORTINOVIS, D. KRESSNER, AND Y. NAKATSUKASA, *Speeding up krylov subspace methods for computing via randomization*, SIAM Journal on Matrix Analysis and Applications, 45 (2024), pp. 619–633.
- [10] B. N. DATTA, *Numerical linear algebra and applications*, SIAM, 2010.
- [11] F. DIELE, I. MORET, AND S. RAGNI, *Error estimates for polynomial krylov approximations to matrix functions*, SIAM journal on matrix analysis and applications, 30 (2009), pp. 1546–1565.
- [12] M. DRISCOLL AND B. DELMOTTE, *Leveraging collective effects in externally driven colloidal suspensions: experiments and simulations*, Current Opinion in Colloid & Interface Science, 40 (2019), pp. 42–57, <https://doi.org/10.1016/j.cocis.2018.10.002>.
- [13] M. EIERMANN AND O. G. ERNST, *A restarted krylov subspace method for the evaluation of matrix functions*, SIAM Journal on Numerical Analysis, 44 (2006), pp. 2481–2504.
- [14] D. L. ERMAK AND J. A. MCCAMMON, *Brownian dynamics with hydrodynamic interactions*, The Journal of chemical physics, 69 (1978), pp. 1352–1360.
- [15] A. FROMMER, S. GÜTTEL, AND M. SCHWEITZER, *Efficient and stable arnoldi restarts for matrix functions based on quadrature*, SIAM Journal on Matrix Analysis and Applications, 35 (2014), pp. 661–683.
- [16] S. GÜTTEL AND M. SCHWEITZER, *Randomized sketching for krylov approximations of large-scale matrix functions*, SIAM Journal on Matrix Analysis and Applications, 44 (2023), pp. 1073–1095.
- [17] W. HACKBUSCH ET AL., *Hierarchical matrices: algorithms and analysis*, vol. 49, Springer, 2015.
- [18] J. M. HERNÁNDEZ-LOBATO, M. W. HOFFMAN, AND Z. GHAHRAMANI, *Predictive entropy search for efficient global optimization of black-box functions*, Advances in neural information processing systems, 27 (2014).
- [19] N. HIGHAM, *Functions of matrices: Theory and computation*, 2008.
- [20] M. ILIĆ, I. W. TURNER, AND D. P. SIMPSON, *A restarted lanczos approximation to functions of a symmetric matrix*, IMA journal of numerical analysis, 30 (2010), pp. 1044–1061.
- [21] D. KIM, T. ZOHDİ, AND R. SINGH, *Modeling, simulation and machine learning for rapid process control of multiphase flowing foods*, Computer Methods in Applied Mechanics and Engineering, 371 (2020), p. 113286.
- [22] N. KISHORE KUMAR AND J. SCHNEIDER, *Literature survey on low rank approximation of ma-*

- trices*, Linear and Multilinear Algebra, 65 (2017), pp. 2212–2244.
- [23] L. LIN, J. LU, AND L. YING, *Fast construction of hierarchical matrix representation from matrix–vector multiplication*, Journal of Computational Physics, 230 (2011), pp. 4071–4087.
 - [24] Z. MA AND W. PAN, *Shape deformation, disintegration, and coalescence of suspension drops: Efficient simulation enabled by graph neural networks*, International Journal of Multiphase Flow, 176 (2024), p. 104845.
 - [25] Z. MA, Z. YE, AND W. PAN, *Fast simulation of particulate suspensions enabled by graph neural network*, Computer Methods in Applied Mechanics and Engineering, 400 (2022), p. 115496.
 - [26] Z. MA, Z. YE, E. SAHDARIAN, AND W. PAN, *\mathcal{H} -HIGNN: A Scalable Graph Neural Network Framework with Hierarchical Matrix Acceleration for Simulation of Large-Scale Particulate Suspensions*, arXiv preprint arXiv:2505.08174, (2025).
 - [27] G. MAKEY, S. GALIOGLU, R. GHAFARI, E. D. ENGIN, G. YILDIRIM, Ö. YAVUZ, O. BEKTAŞ, Ü. S. NIZAM, Ö. AKBULUT, Ö. ŞAHİN, ET AL., *Universality of dissipative self-assembly from quantum dots to human cells*, Nature Physics, 16 (2020), pp. 795–801.
 - [28] C. MUSCO, C. MUSCO, AND A. SIDFORD, *Stability of the lanczos method for matrix function approximation*, in Proceedings of the Twenty-Ninth Annual ACM-SIAM Symposium on Discrete Algorithms, SIAM, 2018, pp. 1605–1624.
 - [29] Y. NAKATSUKASA AND J. A. TROPP, *Fast and accurate randomized algorithms for linear systems and eigenvalue problems*, SIAM Journal on Matrix Analysis and Applications, 45 (2024), pp. 1183–1214.
 - [30] D. PALITTA, M. SCHWEITZER, AND V. SIMONCINI, *Sketched and truncated polynomial krylov methods: Evaluation of matrix functions*, Numerical Linear Algebra with Applications, 32 (2025), p. e2596.
 - [31] G. PLEISS, M. JANKOWIAK, D. ERIKSSON, A. DAMLE, AND J. GARDNER, *Fast matrix square roots with applications to gaussian processes and bayesian optimization*, Advances in neural information processing systems, 33 (2020), pp. 22268–22281.
 - [32] R. T. POWERS AND E. STØRMER, *Free states of the canonical anticommutation relations*, Communications in Mathematical Physics, 16 (1970), pp. 1–33.
 - [33] Y. SAAD, *Iterative methods for sparse linear systems*, SIAM, 2003.
 - [34] R. C. THOMPSON, *Principal submatrices ix: Interlacing inequalities for singular values of submatrices*, Linear Algebra and its Applications, 5 (1972), pp. 1–12.
 - [35] D. S. WATKINS, *Fundamentals of matrix computations*, John Wiley & Sons, 2004.
 - [36] J. G. WENDEL, *Note on the gamma function*, The American Mathematical Monthly, 55 (1948), p. 563.
 - [37] T. YANG, B. SPRINKLE, Y. GUO, J. QIAN, D. HUA, A. DONEV, D. W. MARR, AND N. WU, *Reconfigurable microbots folded from simple colloidal chains*, Proceedings of the National Academy of Sciences, 117 (2020), pp. 18186–18193.